PAPER • OPEN ACCESS

Comparison of aerosol spectrometers : accounting for evaporation and sampling losses

OPEN ACCESS
IOP Publishing
Measurement Science and Technology
Meas. Sci. Technol. **35** (2024) 045301 (14pp)
https://doi.org/10.1088/1361-6501/ad1b9e

Comparison of aerosol spectrometers : accounting for evaporation and sampling losses

Xavier Lefebvre[1,*], **Antonella Succar**[1], **Emilie Bédard**[2], **Michele Prévost**[2] and **Etienne Robert**[1]

[1] Department of Mechanical Engineering, Polytechnique Montréal, 2500 Chem. de Polytechnique, Montréal, QC, H3T 1J4, Canada
[2] Department of Civil Engineering, Polytechnique Montréal, Montréal, QC, Canada

E-mail: xavier.lefebvre@polymtl.ca

Received 28 September 2023, revised 20 December 2023
Accepted for publication 5 January 2024
Published 12 January 2024

Abstract

Measuring aerosol size distribution with precision is critical to understand the transmission of pathogens causing respiratory illnesses and to identify risk mitigation strategies. It is however a challenging task as the size of pathogen-carrying particles evolves over time due to evaporation. Although measurement techniques well established in the field of aerosol science are often used to characterize bioaerosols, their performance is seldom assessed with respect to evaporation and deposition in sampling lines. Four instruments providing aerosol size distribution were compared using oil and water-based particles. They each rely on different measurement principles: phase doppler anemometry, light scattering, electrical mobility and aerodynamic impaction. Size distributions of oil-based particles showed consistency across different measurement instruments, but significant discrepancies arose for water-based particles undergoing evaporation. These larger differences result from both evaporation and particle deposition in transit between the sampling point and the measurement inside the instrument. Phase doppler anemometry was best suited for precise size distribution measurement, as it eliminates the need for a sampling line, thereby preventing particle loss or evaporation during transit. With this instrument as a reference, empirical correction factors for evaporation and deposition were derived from dimensionless numbers and experimental data, enabling quantitative assessment of bioaerosol size distribution using different instruments. To obtain the size distribution at the source of the aerosol generation, complete drying of a salt solution was performed. Using the complete drying technique and accounting for losses, sampling instruments can reliably provide this critical information and allow for thorough risk assessment in the context of airborne transmission.

Supplementary material for this article is available online

Keywords: aerosol characterization, particle deposition, evaporation, size distribution, multiphase flow, stokes number, sherwood number

* Author to whom any correspondence should be addressed.

1. Introduction

The ability of aerosol particles to carry pathogens has been known for over a century [1] and their role as a means of infection has since been the subject of a sustained research effort. The COVID-19 pandemic has highlighted the need to improve our understanding of pathogen dissemination to effectively prevent outbreaks [2]. Potentially infectious aerosol particles settle slowly or not at all depending on their size and on the air flow of indoor environments [3]. These droplets, dependent upon environmental conditions, will gradually lose part of their water content and shrink down to a small nucleus containing the solid matter initially comprised in the droplet, including potential pathogens [4]. Since most bioaerosol particles are water-based, they experience a decrease in size through evaporation immediately following their separation from the bulk solution, unless relative humidity is 100%, in which case particles grow [5]. Such sub-micron droplet nuclei can travel further from the source, remaining airborne until actively removed through ventilation systems [6], and can penetrate deep in the airways when inhaled. Measuring aerosol size distribution accurately is critical to predict the deposition site of particles within the respiratory tract, the size and dose of pathogens they contain, to improve the understanding of their dispersion in ambient air, as well as their settling and deposition dynamics, and to assess the performance of aerosol control procedures or tools. Recent investigations have demonstrated that even small differences in particle size can have a major effect on the behavior of pathogen-carrying particles in indoor air, in the airways and in aerosol treatment systems, especially in the sub-micron range [7–9].

Aerosol size distribution can be measured with a wide variety of instruments relying on different operating principles [10, 11]. The instrumentation currently used in experimental studies of bioaerosol particles consists mainly of impactors and filters [12]. These choices are motivated by the need to obtain cultivable samples and the typically low biological content in air, requiring large volumes to be sampled. However, filters and impactors provide only limited information on the size of the particles carrying pathogens in bioaerosol, and mostly do so when implemented in cascade arrangements that are cumbersome to use.

Risk assessment infection models require the estimations of the number of particles, their size distribution and their configuration-specific drying profile [13]. Research groups working with bioaerosol particles have explored the use of precise analytic tools to get this critical information, that can quickly and conveniently provide detailed particle size distributions [14, 15] but are unable to capture culturable samples. As different physical phenomena are involved with each instrument, there is a need to provide guidelines for meaningful interpretation of experimental data combining size distribution information and the detection of pathogens.

In this study, a transversal comparison between four instruments using different measurement techniques is performed. Two optical instruments are used: a phase Doppler anemometer (PDA) that detects single particles going through a measurement volume without sampling air [16], and a portable optical aerosol spectrometer (OAS) (GRIMM mini LAS 11-R) [17]. Detailed sub-micron size distributions are also obtained through the electrical mobility of particles using a Scanning Mobility Particle Sizer (SMPS) [18]. Finally, a Cascade Impactor is used to obtain the size distribution through the aerodynamic diameter of particles [19], a method adopted in most bioaerosol studies where the particle size is obtained [20]. As wet aerosol size changes dynamically due to evaporation, measurements are conducted on both drying and non-drying aerosol droplets.

The main objective of this study is to improve our understanding of the deposition in the transit and the drying behavior of water-based droplets in common aerosol spectrometers, using four different experimental approaches. First, a comparison is performed using oil-based and water-based particles suspended in air. Second, the effects of evaporation and deposition on the size distribution are studied using an OAS and a PDA with water-based droplets. Third, correction factors are defined to adjust the size distribution measurements of multiphase flows experiencing evaporation and deposition during transit, according to a reference instrument. Lastly, a technique is implemented based on the dried particle size distribution obtained from a saline solution, enabling the calculation of the initial diameter of the particles. These results allow for the use of cost-effective and portable spectrometers to achieve a more accurate estimation of the size distribution at a specific location. Therefore, the outcomes presented in this study serve as a valuable reference for characterizing droplets containing pathogens in a scientific context.

2. Methodology

2.1. Aerosol generation

As droplet size for volatile liquids can change rapidly due to evaporation, measurements were conducted on both drying (water-based) and non-drying (Di-Ethyl-Hexyl-Sebacate (DEHS) oil-based) aerosol droplets. The four aerosol spectrometers considered were first compared using particles produced by a TOPAS GMBH model ATM 221 aerosol generator. This instrument can be operated with water, a saltwater solution or DEHS oil, generating a stable distribution of particles in the sub-micron range. The size distribution generated from this type of instrument fluctuates by a maximum of 2.5% over several hours of use [21]. Aerosol particles generated with DEHS, which has a density of 0.9 $\mathrm{g\,cm^{-3}}$, are spherical and serve as a control for the aerosol emission size, as they dry very slowly over the course of a few hours. During operation, the aerosol generator was connected to a mass flow controller (Hastings HFC 202), enabling regulation of the output flow rate of aerosol in the 0–25 standard liter per minute (SLPM) range.

The instruments were then compared using aerosol particles produced by a spray gun (1.0 mm Mini HPLV Air Spray Gun, Neiko) utilizing tap water. The spray gun, operated with 6 bars of pressurized air, yielded larger particles

in comparison to the TOPAS aerosolizer and was more suitable for covering the entire size range of the measurement instruments employed in the study.

The last experiment was conducted with a solution of 10% m/m NaCl (density of 2.16 $g\,cm^{-3}$) dissolved in tap water, aerosolized with the spray gun. For saltwater-based measurements, aerosol particles were completely dried with a desiccator column filled with silica gel beads (Model DDU 570, TOPAS GMBH). The use of high salt concentration ensured the presence of a detectable nucleus after drying.

2.2. Aerosol characterization

2.2.1. Phase doppler anemometry (PDA). The phase doppler anemometry (PDA/LDA system, Dantec Dynamics, Skovlunde, Denmark) technique is an extension of laser doppler anemometry. The measurement volume is defined by the intersection of two pairs of laser beams with wavelengths of 532 and 561 nm. As single particles flow through the measurement volume, light is scattered from the interference patterns created by the two laser beam pairs [16]. The particle velocity is obtained from the doppler shift of the interference fringes, while information on its size can be acquired from the phase shift. Since the measurement volume is very small, measurements are considered punctual, distinguishing the PDA from the other instruments, making it ideal for the measurement of spray particles [22]. The measurement size range was from 0,5 µm to 8000 µm for the instrument used in this study. Specific settings (appendix), were selected to ensure that the maximum number of particles were detected by the PDA, without saturating the detectors. The PDA measurements, being made directly in the region of the flow where the aerosols are sampled for the other instruments, are used as reference.

2.2.2. Optical aerosol spectrometer (OAS). An optical aerosol spectrometer (OAS) (MiniLAS model 11-R, GRIMM Aerosol Technik Ainring GmbH & Co, Ainring, Germany), is an optical instrument that measures the light scattering of single particles with a diode laser to obtain the size distribution of an aerosol [17]. It is usually employed for atmospheric measurements. However, when used to characterize the size distribution in a flowing aerosol, it is common to connect a sampling tube to the inlet of the instrument [23, 24].

For this study, a 1.5 m sampling tube, of which the smallest section was 2 mm in diameter, was connected at the inlet of the instrument for particle measurements. It is recognized that employing a long sampling line may lead to sampling losses [25]. However, the functionality of the instrument was dependent on the use of a sampling line in the studied configuration and the objective was to evaluate and compare instruments under conditions that accurately reflect their typical use for bioaerosol [26–28]. The inlet sampling flow rate was set at 1.2 l min^{-1}. Particles with a size ranging from 0.25 to 32 µm were measured. The instrument requires knowledge of the particle density for mass distribution measurement. Repetitive measurements were taken every 6 s for 5 min and averaged in a single size distribution.

2.2.3. Scanning mobility particle sizer (SMPS). The scanning mobility particle sizer (model 3938 L76, TSI Incorporated, Shoreview, MN, USA) used in the study, hereafter called SMPS, consists of a differential mobility analyzer (DMA model 3081A) and an ultrafine condensation particle counter (CPC model 3736), which is butanol-based [18]. In the DMA, the particles are drawn to an electrically charged rod at different rates as a function of their size, only letting one narrow particle size range go through to the CPC. The condensation particle counter finally counts the particles of each size and creates the size distribution.

Extensive literature, including studies by Wang and Flagan [29] and Watson *et al* [30], underscores the reliability of SMPS measurements, with any discrepancies between water-based and calibration aerosols predominantly manifesting in the 10–30 nm range, deemed too small to be relevant in the context of airborne transmission. Therefore, deviations in the measurement efficiency of the SMPS were neglected for the size range considered here.

The DMA was fitted with a 71 µm impactor nozzle and a flow rate of 1.2 L/min was drawn with a sheath flow rate of 2.0 L/min. The scanning time was 60 s, the retrace time was 6 s and the purge time was 10 s, which yielded a total time of 76 s for each measurement. These settings resulted in a diameter measurement range of 22 nm–671 nm. The samples were drawn through plastic tubes of 4 mm in diameter connected to a 2 m flexible silicone tube (TSI Conductive Silicone Tubing) at the inlet of the instrument. Results are presented with diffusion correction applied in the software. Repetitive measurements were performed every 2 min for a total of 3 scans, averaged in a single size distribution. The impactor nozzle was cleaned between every set of 3 scans.

2.2.4. Cascade Impactor. The aerosol flow was also measured with a Cascade Impactor (Dekati Low Pressure Impactor DLPI+). Particles with sizes ranging from 0.16 to 10 µm were collected on 14 different stages based on their aerodynamic diameter, with a sampling flow rate of 10 L/min for 30 minutes. The size associated with each stage is a D50 value, implying that each particle with a given size or larger is collected with 50% efficiency. The larger particles have more inertia and are collected on the first stages while the smaller particles have less inertia and are found on the lower stages. The samples were drawn through a flexible plastic tube with a diameter of 12.7 mm and a length of 0.6 m. Each stage was cleaned with ethanol and water, and weighed before and after measurements. Number size distribution was then derived from the mass of particles collected on each stage, assuming sphericity and constant density.

The time delay between sampling and weighing was approximately 3 to 5 min. While the evaporation of DEHS droplets is negligible over this timeframe [31], for water-based droplets, substantial evaporation occurs, leaving only suspended and dissolved solids for mass measurement. To address

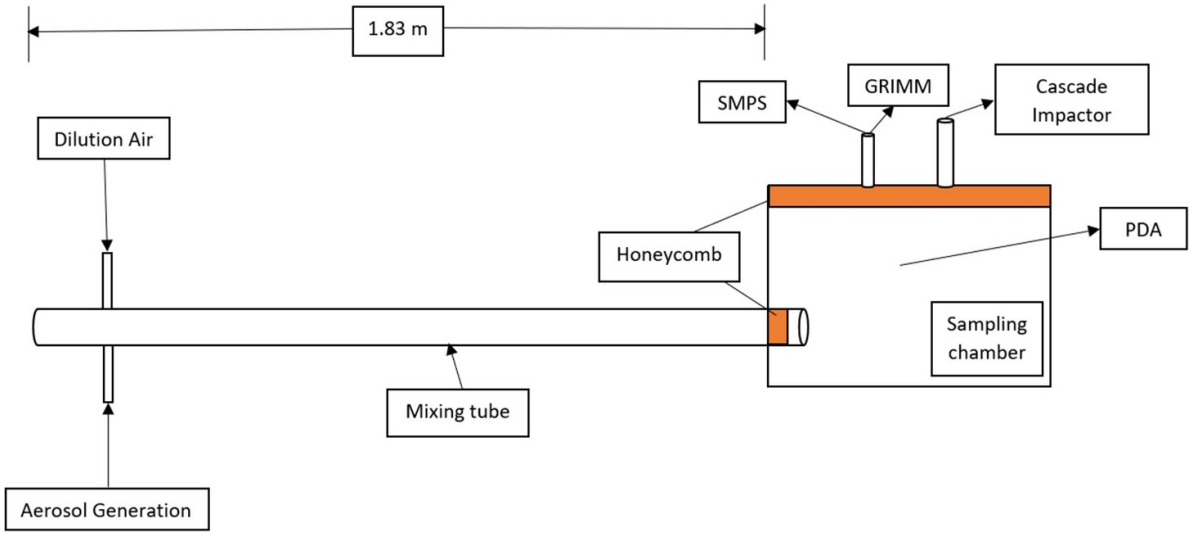

Figure 1. Schematic representation of the experimental facility.

this challenge, it was assumed that evaporation was complete and that the remaining solid particles were spherical, with their individual mass obtained from the characteristics of the stage considered. The assumption of complete evaporation was confirmed by visual inspection prior to weighting, although some water could remain in the particles at the moment of impaction.

2.3. Experimental facility

The experiment aimed at diluting aerosol particles with clean air to produce a well-mixed and low-speed flow into a sampling chamber common to all instruments (figure 1). To enable the comparison of the size distribution measured with each instrument using the same aerosol, it was necessary to dilute with clean air to avoid saturation. The low flow speed into the sampling chamber and a sampling tube diameter adapted to each instrument flow rate resulted in equal velocities between the air around and inside the tube, which minimized the divergence of the flow lines at the sampler inlet [32]. This isokinetic condition prevents skewed size distribution measurements due to the inertial effects of particles entering the sampling tube. The sampling chamber had a volume of 53 L and was made of clear polymethyl methacrylate (PMMA, plexiglass) so that the optics of the PDA could measure particles through the side walls. Honeycomb material was fixed at the inlet and outlet of the mixing chamber to dampen large flow structures. During the measurements, the mean temperature in the laboratory was 25 °C and the mean relative humidity was 42%.

For DEHS aerosol particles, the injection of aerosol particles was done perpendicularly to the longitudinal direction of the tube and set by the flow controller at 4.2 L/min, for a dilution ratio of 1:5. The clean dilution air was injected from the other side of the tube, in the same manner as the aerosol. By injecting the particles and the air perpendicularly from the longitudinal direction of the tube, turbulence is created, and promotes the mixing of the two flows. To ensure that the flow was properly mixed and that a steady state concentration was reached, a tube of length 1.83 m with an inside diameter of 0.0762 m was used between the aerosol inlet and the sampling chamber ($L/D = 24$). Measurements were also started 3 min after flow initiation. Following every measurement, the chamber was drained by turning off the aerosol generator and injecting compressed air at 6.6 L/min for 10 min. For all experiments, the measurements were replicated three times to assess repeatability.

2.4. Aerosol drying

Aerosol generation from DEHS was ideal for instrument comparison since the particles only dry over several hours in ambient conditions. Additionally, NaCl water-based aerosol particles were used to study evaporation. The use of a sampling line was investigated by comparing the size distribution measured by the OAS and the PDA, using the spray gun and salt water to generate larger aerosol particles compared to those obtained from DEHS in the TOPAS instrument. To remove the complexity associated with uneven evaporation for size distribution measurement, the droplets were also completely desiccated and measured from the sampling chamber with the SMPS. The SMPS was used because dried particles are smaller and in the appropriate size range for measurement with this instrument. The size distribution was also measured without using the desiccator, for comparison.

Knowing the concentration of salt per volume of the water solution C_s $(\mathrm{kg\,m^{-3}})$ as well as the measured mass of salt per volume of air M_f $(\mathrm{kg\,l_{air}^{-3}})$, with the sampling flow rate $\dot{V}$ $(\mathrm{l_{air}^{-s}})$ and the measurement time t (s), the total volume of water for each size bin V $(\mathrm{m^3})$ can be calculated

$$V = \frac{M_f \dot{V} t}{C_s}. \tag{1}$$

Then, knowing the number of particles for each size bin n, the diameter of the particles generated at the source D_s (m),

was derived, assuming that the transfer rate of NaCl from the solution to the aerosol particles was constant and that the generated droplets were spherical. The source size distribution was then reconstructed from the diameter at the source for each size bin

$$D_s = \sqrt[3]{\frac{6V}{n\pi}}. \tag{2}$$

2.5. Number concentration

To account for the fact that the number of size bins is not the same for every instrument, and that the bins are unequal in width, the y-axis on size distribution plots is normalized by dividing the number concentration of each bin by the logarithm of the bin width [33]. This results in a log-normal distribution. Some instruments such as the SMPS already provide a normalized size distribution, but for the OAS, the Cascade Impactor and the PDA, the concentration had to be normalized through data post-treatment. While the OAS and the SMPS produce the size distribution by volume of air sampled, the PDA only counts the number of particles passing through the measurement volume and the cascade impactor yields the cumulative mass of the particles collected on each stage. The particle concentration per liter of air N_C therefore needs to be calculated in the case of the PDA and the cascade impactor. For the latter, since the measurement was made over 30 min and the flow is pumped at a constant rate of 10 l s−1, the mass concentration was obtained for each stage by dividing the accumulated mass M $(\mathrm{kg/L_{air}})$ by the sampling flow rate $\dot{V}$ $(\mathrm{1s^{-1}})$ and the time of measurement t (s). The number concentration was then calculated assuming sphericity and constant density ρ_p $(\mathrm{kg/m^3})$, where V_p $(\mathrm{m^3})$ is the volume of one particle of the measured size

$$N_C = \frac{M}{\rho_p V_p \dot{V} t}. \tag{3}$$

For the PDA, the cross-section of the measurement volume perpendicular to the flow represents the measurement surface needed to calculate the volume of gas covered by the laser. The measurement volume provided by the supplier was verified by laser irradiance measurement [34], and confirmed at 2.6 mm by 153.1 µm. Assuming that the measurement volume is ellipsoidal, the measurement surface could be derived. The speed of the flow through the measurement volume is known, as the instrument also provides particle velocity, and the time of the measurement remains constant. The concentration of particles per liter of air N_P can therefore be obtained by dividing the counted particle number N by the mean flow velocity V_m (m/s), the time of measurement t (s) and the measurement surface S $(\mathrm{m^2})$

$$N_P = \frac{N}{S V_m t}. \tag{4}$$

The SMPS and PDA distributions are composed of 100 size bins, while the OAS and the Cascade impactor only produced size distributions with 9 and 6 bins, respectively, for the DEHS measurements. The size resolution improved slightly for water-based droplets with respectively 11 and 7 bins used for the latter two instruments.

3. Results and discussion

3.1. Instruments comparison

The size distributions of oil-based and water-based droplets were measured and compared with the OAS, the SMPS, the PDA and the Cascade Impactor (figure 2). The peak concentration of DEHS particles in the air was found to be approximately 6×10^7 for all the instruments. However, the water-based measurements showed a wider range of peak concentrations, varying between 10^7 and 10^9 particles per liter of air. The modes of DEHS particles coincided for all instruments at approximately 0.3 µm with a variance a thousand times smaller than for the water-based measurements. Essentially, the size distribution statistically concurred for the measurement of DEHS droplets but not for water-based droplets and the discrepancies between both configurations are significant according to a T-test conducted on the modes of the distribution ($p < 0.05$).

OAS and SMPS spectrometers as well as the cascade impactor require the use of a small inlet sampling tube, in which some particles may be lost by impaction on the walls or through evaporation. The use of a sampling line was investigated further by comparing the size distribution obtained from the spray gun with the PDA and the OAS (figure 3(a)). In addition to the expected losses in measurement associated with particle deposition, it was observed that the size distribution of the OAS was shifted towards smaller particles. This shift indicated that the measurement process was also affected by evaporation, which occurred rapidly as the particles went through the sampling line (transit time of 1.16 s). Therefore, deposition and evaporation of particles are likely responsible for the significant discrepancies observed within the size distribution measurements conducted with instruments using different working mechanisms and their effects must be considered.

Evaporation does occur between the generation and sampling site and is of significant interest in the context of airborne transmission. However, the primary objective of this study aimed to offer a practical comparison of aerosol size distribution measurement instruments under consistent laboratory conditions. As such, the evaporation considered here pertains specifically to the interval from the sampling point to the measurement point inside the instrument. Thus, the measurement volume of the PDA could be considered as the source and coincident with the sampling point of the other instruments.

As the sampling flow rate through the different instruments is generally fixed (except for the SMPS for which a slight adjustment is possible), the sampling tube diameter is imposed

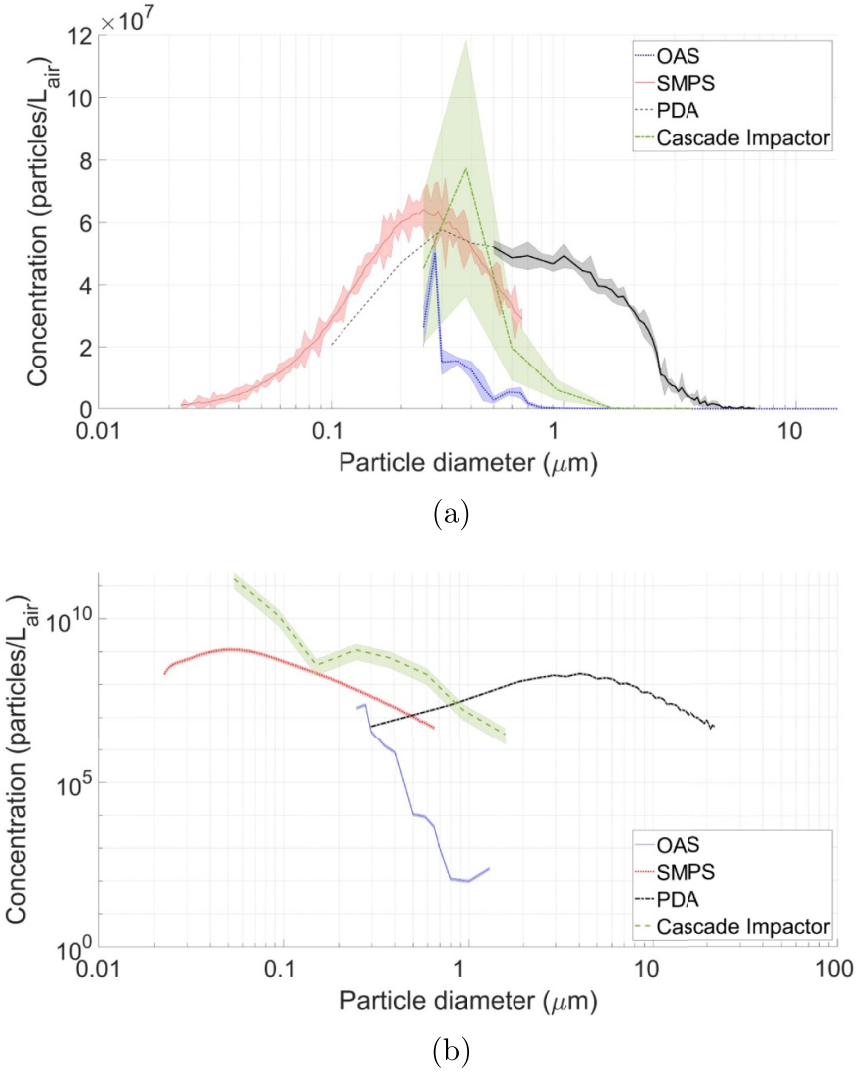

Figure 2. Comparison of the size distribution measurements from the four instruments (a) with DEHS aerosol particles. (b) with water-based aerosol particles. Results are averaged over three measurements. Shaded areas show the standard deviation within repeated runs.

to achieve isokinetic sampling. When comparing the concentration measured by the different instruments, the OAS measured up to 5 orders of magnitude fewer particles than the other instruments (figure 2 (a). For particles larger than 0.25 μm, differences in the measurement were at least 40%, and from 0.8 μm, reached close to 100%, revealing that larger particles are less likely to be detected by the OAS (figure 3(b)). Some particles are lost, others evaporate in transit and are detected at a lower size. This effect appears mostly significant with the OAS. However, as the mode and shape of the distribution were qualitatively in agreement, the results provided by this highly portable instrument remain valuable, especially when measuring either dry or slowly evaporating particles.

Due to the lower resolution inherent in its measurement principle, the cascade impactor showed the highest variability in the measurements (figure 2). In effect, the use of cascade impactors to characterize the size distribution of droplet-laden flows poses significant challenges due to the inherent evaporation of droplets during sampling, following impaction and prior to mass measurement. This temporal gap introduces uncertainties, particularly for water-based droplets, as evaporation of the deposited droplets is significant. To mitigate this issue, assumptions were made to assume total evaporation and treat the remaining solid particles as spherical entities. While cascade impactors offer benefits in capturing particles based on their aerodynamic size, the limitations associated with evaporation and the subsequent conversion process make them suboptimal instruments for achieving precise size distribution characterization in the context of droplet-laden flows.

The PDA displayed among the most repeatable measurements and detected larger and more particles than the other instruments in all investigated configurations, since it does not require a sampling tube, minimizing evaporation and losses in the sampling line. Therefore, the PDA can be regarded as a reference over its size range. However, since the wavelengths of the lasers used in the PDA are approximately 0.5 μm, the measurements for smaller particles lacked precision, and are therefore illustrated as a dashed line. For particles smaller than 0.5 μm, the SMPS is considered the gold standard as very little losses are expected in transit for such small particles.

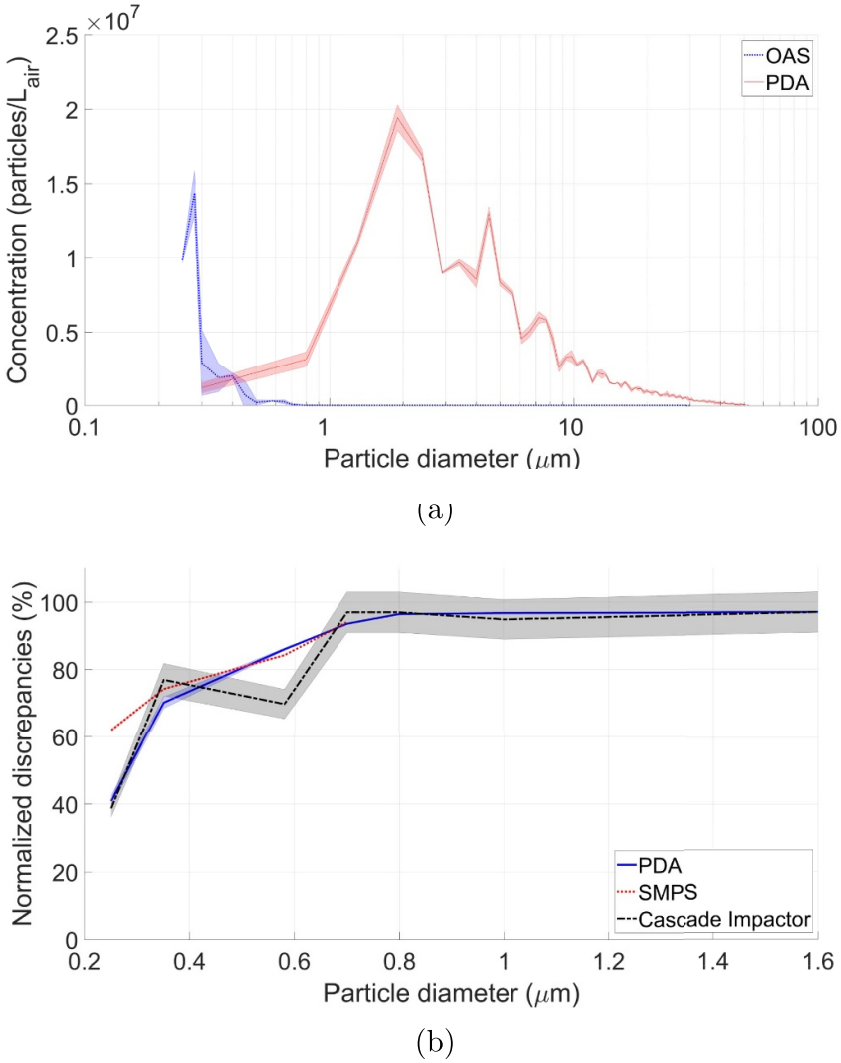

Figure 3. (a) Comparison of the OAS and the PDA to show the effect of the sampling tube on the measurements. Results are averaged over three measurements. Shaded areas show the standard deviation within repeated runs. (b) Sampling discrepancies observed with the OAS compared to the other three instruments.

Decripancies arose within the size distribution measurements of both water-based and oil-based particles from different instruments. Although much slower than for water evaporation also occurs in oil-based particles, and the effect of particle deposition could be observed for the measurement of larger oil-based particles from the OAS and the cascade impactor. However, the effects of evaporation and particle deposition on the size distribution measurements were more significant for water-based particles because of their combined effect. The fact that evaporation was negligible for DEHS measurements [31] explains the much better agreement between the instrument than for water-based droplets, as only the effect of particle deposition caused the measurement discrepancies. As such, sections 3.2–3.4 will focus on the development of empirical correction factors, with the PDA as a reference, for configurations where evaporation and deposition in sampling lines are occurring.

3.2. Evaporation

The evaporation of the measured particles can be characterized by the dimensionless Sherwood number, which represents the ratio of the convective mass transfer h ($\mathrm{m\,s^{-1}}$) to the mass diffusivity D ($\mathrm{m^2/s}$). With knowledge of the particle diameter d_p (m), the Sherwood number can be calculated [35] :

$$Sh = \frac{h}{D/d_p}. \tag{5}$$

While the Sherwood number itself may not explicitly include terms for temperature and relative humidity, the convective mass transfer coefficient (h) it includes is influenced by these ambient conditions [35]. The convective mass transfer coefficient h ($\mathrm{m\,s^{-1}}$) is a function of the surface of the droplet A ($\mathrm{m^2}$), the molar mass transfer $\dot{n}_A$ ($\mathrm{mol\,s^{-1}}$) and the vapor

concentration difference between the boundary surface and the ambient air Δc (mol m^{-3}):

$$h = \frac{\dot{n}_A}{A\Delta c}. \tag{6}$$

Therefore, changes in temperature and relative humidity in the atmosphere can indirectly affect the Sherwood number and, consequently, the mass transfer characteristics of aerosol droplets during evaporation.

The mass diffusivity coefficient can be easily derived for DEHS and water with respect to ambient air, knowing the relative properties of the interacting fluids. As for the convective mass transfer coefficient h, it is a function of the mass transfer rate at the interface of the droplet, the area of the interface and a driving force coefficient, which is dependent upon the conditions, and complex to infer. However, using dimensional analysis for the evaporation of a spherical droplet, the Sherwood number can also be defined as the Froessling function, dependent upon the Reynolds and Schmidt numbers [36]. With knowledge of the density of the fluid ρ (kg m^{-3}), the dynamic viscosity of the fluid μ (kg ms^{-1}), and the velocity of the particles relative to the air u (m s^{-1}), it was calculated here using the following equation :

$$Sh = f(\mathrm{Re}, \mathrm{Sc}) = 2 + 0.552\,(\mathrm{Re})^{\frac{1}{2}}\,(\mathrm{Sc})^{\frac{1}{3}} \tag{7}$$

where

$$\mathrm{Re} = \frac{\rho u d_p}{\mu}; \mathrm{Sc} = \frac{\mu}{\rho D}.$$

The rate of evaporation I (kg/s), characterized as the loss of water m (kg) over time t (s), is linearly proportional to the surface area of a liquid droplet of and thus to the square of the droplet diameter d (m) [35].

$$I = \frac{-m}{t} \propto \pi d^2.$$

Therefore, a correction factor for the evaporation of droplets before they are measured needs to consider the square root of the transit time (t). Also, although very slow due to the nature of the fluid, evaporation does occur for DEHS droplets. Because DEHS is used as a reference for evaporation, the correction factor must consider the Sherwood numbers of both oil-based (Sh_{DEHS}) and water-based droplets (Sh_{water}). Finally, the properties of the fluids and the aerosol generation mechanism influence the size of the generated droplets. As such, the correction factor must include the ratio of the modes of the water-based size distribution ($D_{p;m,\mathrm{water}}$), over the DEHS size dsitribution ($D_{p;m,\mathrm{DEHS}}$). In light of all these hypotheses, the following empirical correction factor can be used to adjust for the bias of the droplet diameters measured due to evaporation:

$$K_{\mathrm{evap}} = \frac{D_{p;m,\mathrm{water}}}{D_{p;m,\mathrm{DEHS}}\sqrt{t}}\frac{Sh_{\mathrm{DEHS}}}{Sh_{\mathrm{water}}}. \tag{8}$$

The transit time t was calculated by dividing the volume of the sampling line (m^3) by the sampling flow rate (m^{3}s^{-1}). The PDA was used as the reference instrument. As such, the correction factor was applied respectively to each of the particle sizes for all the instruments except for the PDA, and the correction factor incorporated the ratio of the modes from the size distribution of different fluid, measured with the PDA. As an example with the OAS, a transit time of 1.16 seconds, Sherwood numbers of 36.13 and 32.86 respectively for DEHS and water and the ratio of the modes of 13.33, yielded a correction factor K_{evap} of 13.60. For a particle size of 0.5 µm measured with the OAS, the corrected particle size was therefore 6.8 µm (figure 5).

3.3. Sampling line deposition

The deposition of particles on the walls of the sampling line, resulting in measurement losses, can be characterized by the Stokes number and the length of the sampling line. The Stokes number quantifies the capacity of the particles to follow the streamlines of the flow. The length of the sampling line affects the particle essentially through the transit time available for deposition to occur. Sampling line deposition of particles mostly influences the measured concentration, which is not affected equally for all droplet sizes, as larger particles, with a larger Stokes number, exhibit a higher propensity for settling and colliding with the walls. Both the length of the sampling tube and the Stokes number can be combined in a single parameter [37]. However, in this section, we will assess the effect of both phenomena on the measurement separately.

3.3.1. Particle transit. The likelihood of particle loss through settling in the sampling line during transit, before reaching the measurement point of the instrument, can be characterized by the dimensionless Stokes number, which is the ratio of the characteristic time of a particle t_0 to the characteristic time of the flow. Knowing the particle density ρ_p (kg m^{-3}), the diameter of the particles d_p (m), the dynamic viscosity of the air μ_g (kg ms^{-1}), and the flow speed u (m s^{-1}), the Stokes number is defined as :

$$Stk = \frac{t_0 u}{d_p} \tag{9}$$

where

$$t_0 = \frac{\rho_p d_p^2}{18\mu_g}.$$

For large particles, the Stokes number is therefore large and impaction on the sampling line walls, which are bound to include bends, is more likely to occur because of the inertia of the particles. The flow rate was 1.2 l min^{-1} in the sampling line of the OAS, 2.0 l min^{-1} for the SMPS and 10 l min^{-1} for the cascade impactor. For a 0.5 µm particle, this resulted in Stokes number of 9.8×10^{-3}, 4.1×10^{-3} and 2.02×10^{-3}, respectively, inside the sampling lines of the OAS, the SMPS and the cascade impactor. The Stokes number for OAS measurements was more than twice that of the SMPS and was five times larger than that of the cascade impactor, explaining the

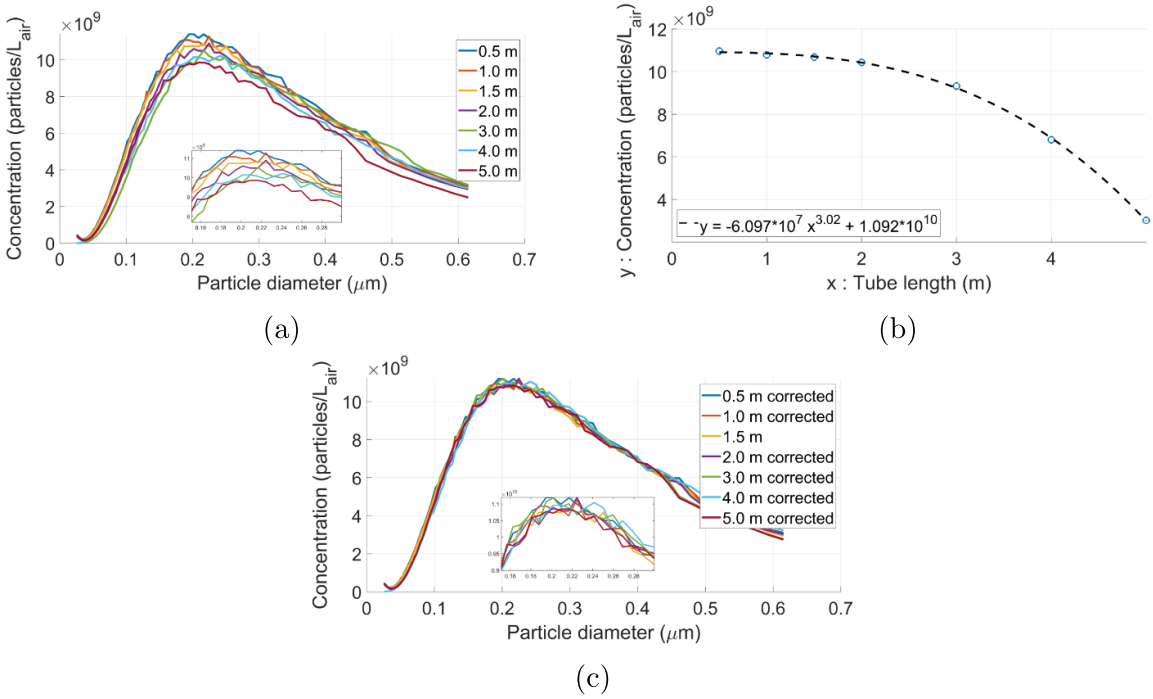

Figure 4. (a) Average of SMPS measurement triplicates of the concentration as a function of droplet diameter for five sampling tube lengths (0.5, 1.0, 1.5, 2.0, 5.0 (m). (b) Curve fitting of the concentration (y) as a function of the tube length (x), for the mode of the size distribution. (c) Corrected size distribution according to the sampling line length with reference to the 1.5 m sampling line.

losses in the sampling line for larger particles with the former. The differences here were exacerbated by the fact that these losses are strongly size dependent, as well as the ability of the OAS to detect much larger particles, up to 32 µm.

The Stokes number (Stk) depends on the droplet diameter and is therefore size specific. Thus, a correction factor for particle deposition inside the sampling line must affect the concentration differently depending on the particle size, the droplet fluid and the measurement instrument used. For a specific particle diameter, the Stokes number varies linearly with the properties of the fluid, so the correction factor is expected to be a linear function. Also, particle deposition occurs regardless of the fluid, but the properties of the fluid making up the droplets influence the behavior of the particles. Consequently, the correction factor should include the ratio of the density of DEHS and water as well as the viscosity of the ambient air. The following empirical correlation can therefore be used to correct the bias of the droplet concentration measured due to particle deposition :

$$K_{\text{dep}} = \alpha Stk \tag{10}$$

where

$$\alpha = \frac{0.87}{\mu_{\text{air}}} \frac{\rho_{\text{DEHS}}}{\rho_{\text{water}}} = 4285.$$

In the correction factor, the factor of 0.87 is an empirical value that corrected for the differences in viscosity of the humid air surrounding the aerosol in relation to the ambient air [38]. The correction factor was multiplied by the concentration and was size-dependent. The reference for the calculation of the empirical correlation factor was the PDA, meaning that it was applied to the particle sizes of all the instruments except for the PDA. As an example, approximately 10^4 water-based particles of size 0.5 µm were measured with the OAS per liter of air. The Stokes number was 9.8×10^{-3}, which yielded a correction factor of approximately 42. The corrected particle concentration was therefore 4.2×10^5 particles per liter of air.

3.3.2. Effect of the sampling line length. The length of the sampling tube also affects the measured concentration through measurement losses. Here, the effect of the use of different sampling tube lengths was investigated experimentally, using DEHS particles to avoid the complications associated with evaporation. The size distribution obtained using the SMPS and sampling lines of seven different lengths (0.5, 1.0, 1.5, 2.0, 3.0, 4.0 and 5.0 m) are shown in figure 4 (a). If losses were only the results of inertial effects, the Stokes number reveals that particle deposition should be more significant for larger particles. In the SMPS however, selected based on its suitability for the sub-micron size range investigated, the measurement losses did not exhibit a significant change as a function of the particle size. It was therefore assumed that the correction factor for the sampling line length is not size-dependent.

By using the same measurement instrument, as well as DEHS aerosol droplets to characterize changes in the particle deposition from changes in the length of the sampling line, the resulting observations represent the added probability of particles interacting with the sampling line wall due to its extended length, without the combined effect of evaporation and Stokes number-dependent deposition.

Table 1. Empirical constants for the correction factor of the sampling line length with the SMPS.

Empirical constant	Value
a	-6.097×10^7
b	3.02
c	1.092×10^{10}

The losses in the sampling line were approximately proportional to the cube of the sampling line length L (figure 4(b)). The correction factor for the measurement losses induced by the length of the tube is therefore in the form of a power law with empirical coefficients a, b and c. To correct for the length of the sampling line, the measured concentration can be multiplied by the ratio of the power law applied to the length of the sampling line of the corrected measurement instrument over the length of the sampling line of the instrument used as a reference. As an example, if the SMPS was used a the reference instrument and the size distribution of the OAS was to be corrected, the correction factor would be :

$$K_{\text{lengthSMPS}} = \frac{a\left(L_{\text{OAS}}\right)^b + c}{a\left(L_{\text{SMPS}}\right)^b + c} \tag{11}$$

where table 1 displays the empirical constants.

Applying a single fitting curve corresponding to the mode of the distribution (figure 4(b)) caused minimal disparities when the size distribution measured through the 7 sampling line lengths with the SMPS were corrected (figure 4(c)), especially when compared to the uncorrected measurements (figure 4(a)). This is convenient in this context due to the narrow size range measured using the SMPS.

A better reference to use when correcting for sampling losses is the PDA, which does not use a sampling line. In this case, a proportionality empirical correlation variable β can be used, calculated using the correlation applied to a sampling tube of length zero, multiplied by an empirical constant of 10, acquired through trial and error, which allowed for a better fit. The correction factor can be applied to all instruments covering a wide range of sizes, despite being derived from measurements in the sub-micron size range. The β variable is used to adjust the concentrations to the reference PDA, which is assumed not to be subjected to sampling and evaporation losses, as it performs direct measurements at the location where the other instruments are pulling aerosol. As such, this approach not only allows for a thorough comparison between different instruments, but also provides a means to improve the accuracy of results obtained from affordable tools such the OAS, which costs significantly less than the PDA but is subject to significant sampling and evaporative losses. Considering the PDA as the reference, the best fit for the mode of the concentration of the 7 investigated sampling lengths yielded the following correction factor :

$$K_{\text{length}} = \frac{\beta}{a\left(L\right)^b + c} = \frac{1.0915 \times 10^{11}}{-6.097 \times 10^7 \left(L\right)^{3.02} + 1.092 \times 10^{10}} \tag{12}$$

where

$$\beta = 10\left(a\left(0\right)^b + c\right) = 1.0915 \times 10^{11}.$$

3.4. Corrected comparison

The empirical correction factors presented in the previous sections were applied to the water-based size distribution produced with the spray grun (figure 5). The evaporation correction factor K_{evap} was applied to the particle diameter and the correction factors for the sampling line losses K_{length} and K_{dep} were both applied to the particle concentration. A summary of the correction factors is presented in table 2.

The modes of the corrected size distribution (figure 5) coincide very well, with a droplet diameter of approximately 4 µm, showing that the measured size distribution of water-based particles is not statistically different than that of DEHS particles when corrected with the approach described previously, according to a T-test on the modes ($p > 0.05$). Therefore, the correction factors allow the comparison and combination of measurements obtained from different instruments relying on sampling lines and working with droplets undergoing evaporation.

As observed in figure 2, where disparities in size distribution measurements were identified, the correction factor for evaporation needs to account for particle diameter. This approach was motivated by the significant impact of evaporation on size distribution, particularly for smaller droplets, as substantiated by previous studies [39, 40]. In contrast, the correction factor for sampling line length played a more pronounced role on aerosol concentration, with little effect observed on the particle size (figure 4(a)), for the conditions investigated here. Although a particle size-dependence can be expected for the deposition in the sampling line, with bigger particles depositing more easily, we did not observe such a quantifiable effect for the size range considered here. The correction factors, detailed in table 2, target both evaporation and deposition, acknowledging their preferential effects on size distribution and concentration.

The approach presented here based on correction factors can be adapted to other aerosol sizing measurements relying on sampling. Although the correction factors for evaporation and sampling line losses have been validated for the configuration described in section 2, they can be calculated for different fluid systems or experimental facilities, as they essentially depend on flow conditions and particle characteristics, rather than instrumentation. Conversely, the correction factor for the length of the sampling line requires the availability of a reference instrument such as the SMPS or the PDA. In this study however, the empirical constants of the correction factor were derived from SMPS measurements of submicron DEHS droplets and were then successfully applied to larger water-based droplets measured with different instruments. The results from this investigation can be used to correct experimental data from sampling instrumentation such as optical aerosol spectrometers and impactors similar to those used here.

Finally, the specific measurement instruments used in this study also have their advantages and limitations which can

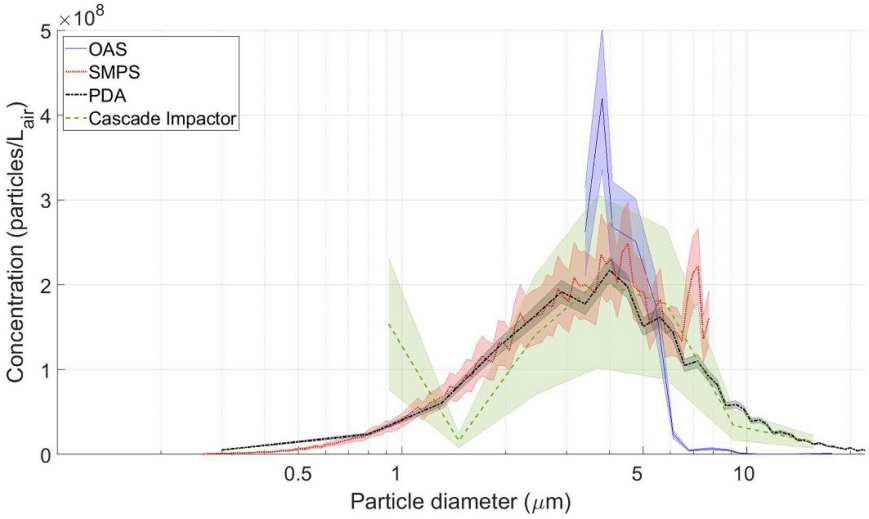

Figure 5. Comparison of the four instruments with water-based aerosol particles corrected empirically. Shaded areas show the standard deviation within repeated runs of the initial measurements.

Table 2. Summary of the correction factors for evaporation, as well as sampling line deposition during particle transit and the length of the sampling line.

Correcting for :	Correction factor	Applied to :
Evaporation	$K_{\text{evap}} = \frac{mo_{\text{water}}}{mo_{\text{DEHS}}\sqrt{t}}\frac{Sh_{\text{DEHS}}}{Sh_{\text{water}}}$	Particle diameter
Sampling line deposition during particle transit	$K_{\text{dep}} = \alpha Stk$ where $\alpha = \frac{0.87}{\mu_{\text{air}}}\frac{\rho_{\text{DEHS}}}{\rho_{\text{water}}}$	Aerosol concentration
Length of the sampling line	$K_{\text{length}} = \frac{\beta}{a(L)^b+c}$ $K_{\text{length}} = \frac{1.0915\times10^{11}}{-6.097\times10^7(L)^{3.02}+1.092\times10^{10}}$	Aerosol concentration

influence the results depending on the application as further discussed in the supplemental material. Applying these correlations to other measurement instruments besides those considered here may also introduce errors due to inherent differences in their measurement principles, as well as their sensitivity and measurement range.

3.5. Circumventing evaporation

The size distribution of NaCl droplets measured with the SMPS, with and without drying the aerosol in a desiccation column (representing the dried and wet distributions respectively), are presented along with the calculated initial size distribution (figure 6). The particle size as they were generated (source distribution) was calculated following the procedure described in section 2, which avoids the complications associated with evaporation during measurement, or between the aerosol source and the measurement point. The concentration at the source was adjusted for the length of the sampling line. The maximum number of particles measured was approximately 2×10^9 particles per liter of air for the dried distribution, and was approximately three times more for the wet distribution, revealing significant particle losses in the drying process.

As expected, the measured particles were much smaller than at the source, due to evaporation. Particles at the source ranged from 0.65 m up to 10 μm and covered a broader range of particles than the dried and wet measurements. 90 % of the generated particles were larger than 1 μm and once measured, all the particles were submicron. This further supports the signficance of the evaporation effect in the measurement process and the importance of considering the measurement biases induced by the use of a sampling line with an evaporating aerosol.

3.5.1. Mass conservation. Following the assumption that the solid concentration in each droplet is equivalent to the bulk solution concentration, it is possible to conduct a mass conservation analysis. Knowing the density of the bulk saline solution used to generate the measured droplets, the total volume of water aerosolized V_t (m^3) can be calculated by integrating the volume of a sphere with the diameter of a measured droplet across the size range of the size distribution at the source, multiplied by the number of measured droplets at that size N_s. The total mass of salt at the source M_s (kg) can then be inferred with the concentration of salt in the bulk saline solution C_s ($\text{kg}\,\text{m}^{-3}$). With knowledge of the measured mass of dried solids M_f (kg), mass conservation calculations can then provide the mass of solids lost during the measurement of the dried particles M_L (kg):

$$M_s = M_f + M_L \tag{13}$$

where

$$M_s = C_s \times V_t$$

$$V_t = N_s \int_{\text{d}_{\text{min}}}^{\text{d}_{\text{max}}} \frac{\pi\,(\text{d}_p)^3}{6}.$$

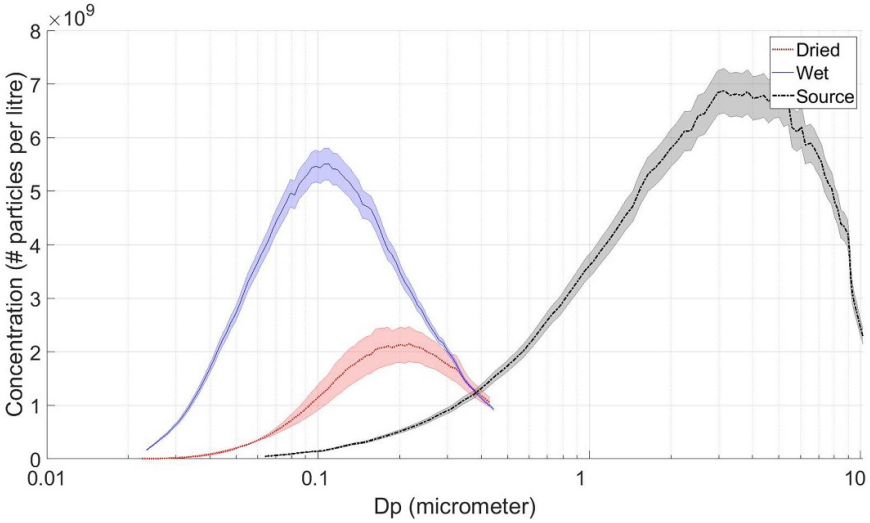

Figure 6. Size distribution from the SMPS with dried NaCl aerosol particles and the calculated size distribution at the source. Results are averaged over triplicate measurements. Shaded areas show the standard deviation within repeated runs.

The mass of the wet size distribution M_w (kg) can also be added to the calculations to isolate the losses in the sampling line and from evaporation M_L^* (kg):

$$M_s = M_w + M_L^*. \tag{14}$$

Approximately 96% of the mass at the source was lost during measurement, attributed to water evaporation, as well as particle deposition in the sampling line and the desiccation column. Particle transit and Stokes number analysis indicated that these measurement losses were significantly exacerbated for larger particles. Wet and dried size distributions only showed a 4% mass difference, suggesting that most losses through evaporation occured during particle transit, reinforcing the key advantage of the PDA as a reference instrument. Water content constituted 90% of the mass at the source, and over 15% of the total mass was lost through sampling line deposition. This entails that evaporation is the dominant factor in the differences between measurements, but that particle deposition also played a significant role. The losses in the desiccation column accounted for less than 5% of all losses, primarily affecting smaller particles due to Brownian motion-induced diffusion during evaporation. This explains the shift towards larger particles in the dried size distribution, where the wet distribution measured with the SMPS had a maximum concentration at a diameter two times smaller than the dried distribution.

3.5.2. Significance of the complete evaporation approach. Research groups focusing on bioaerosols face limitations when using Phase Doppler Anemometry due to safety concerns and practical constraints. Nevertheless, the interest in understanding the size distribution of potentially contaminated droplets remains high. As an alternative, portable and user-friendly instruments like an OAS or impactors are commonly employed. However, these instruments suffer from losses during transit, primarily caused by particle deposition in the sampling line, and evaporation. The incomplete and unknown evaporation process makes the size distribution measurement largely arbitrary and dependant upon environmental conditions. To address this challenge, our approach involves complete evaporation of particles, allowing the calculation of the size distribution at the source by considering the solid content in the bulk solution and after complete drying. However, the significant losses during measurement must be considered. In this study, the PDA was used as a reference to account and correct for these losses. The process of completely drying water-based aerosol particles to then revert to their initial size also demonstrates the possibility of extending this methodology to dry aerosol particles, in that case disregarding the evaporation correction factor.

3.6. Applications

In the context of airborne transmission, the approach outlined also offers a valuable framework for advancing our understanding of respiratory particle dynamics. The choice of appropriate measurement techniques, including a combination of data from several instruments and empirical correction factors for evaporation and deposition, becomes particularly important when applied to the study of aerosols originating from the respiratory system [41]. However, a critical research gap lies in our understanding of aerosol size distribution within the airways themselves [42]. By adapting the methodology proposed here to focus on airway aerosols, a more accurate characterization of size distribution can be achieved, enabling researchers to extract meaningful results from a range of measurement instruments. As such, the use of a sampling line can be valuable to reach specific areas that are difficult to access. Incorporating the correction factors derived in this study can also address potential losses during sampling and

transit. Moreover, the application of a complete drying technique allows for source characterization, providing insights into the initial composition and behavior of aerosols directly from the respiratory system. This comprehensive approach can contribute to a more robust characterization of the risks associated with respiratory pathogen transmission, facilitating the development of targeted mitigation strategies.

4. Conclusions

A transversal comparison was presented between four aerosol size distribution measurement instruments with different working mechanisms, performed in a flow of water and DEHS aerosol particles suspended in the air. Instruments generally agreed when measuring particles that do not evaporate, but not when measuring water-based droplets. For DEHS (oil-based) particles, all instruments detected comparable size distributions and concentrations with minimal differences, except for the OAS, which generally measured at least 70% fewer particles for sizes larger than 0.25 µm, indicating that deposition was also significant for oil-based particles. For water-based aerosol particles, measurement discrepancies affected all the instruments, sometimes exceeding one order of magnitude.

These differences between the measurement of water-based and oil-based particles were explained by the evaporation of water-based droplets before the measurement was conducted, as well as measurement losses due to particle deposition in the sampling line. Empirical correction factors based on the Stokes and the Sherwood numbers, as well as the length of the sampling line were developed to account these measurement biases, using the PDA, which does not use a sampling line, as a reference. These results demonstrate that in the context of airborne transmission, employing size distribution measurement instruments that are not designed for bioaerosol measurements can provide actionable data for proper risk assessment if particle deposition and evaporation are accounted for.

Evaporation was then further investigated by conducting measurements on dried particles and subsequently reconstructing the size distribution at the source. Mass conservation allowed for a quantitative assessment of the measurement losses due to evaporation and deposition. Using this approach, affordable and portable OAS can be used to characterize size distribution at the source if the solid content is known, circumventing difficulties associated with the evaporation process. Therefore, the complete drying of the particles enables the evaluation of the initial size of the generated particles, a critical information in the context of airborne transmission.

Data availability statement

The data cannot be made publicly available upon publication because they are not available in a format that is sufficiently accessible or reusable by other researchers. The data that support the findings of this study are available upon reasonable request from the authors.

Acknowledgments

This research was supported by a NSERC Alliance Grant (ALLRP545363/2019), Polytechnique Montréal. Xavier Lefebvre is supported by the Hydro-Québec excellence scholarship as well as a NSERC scolarship (ES D) with a FRQNT supplement (B2X).

Competing of interests

The authors declare no competing interests.

ORCID iD

Xavier Lefebvre https://orcid.org/0000-0001-7573-0583

References

[1] Horrocks M W H 1906 Experiments made to determine the conditions under which “specific” bacteria derived from sewage may be present in the air of ventilating pipes, drains, inspection Chambers, and sewers *Public Health* **19** 495–506
[2] Shah Y, Kurelek J W, Peterson S D and Yarusevych S 2021 Experimental investigation of indoor aerosol dispersion and accumulation in the context of COVID-19: effects of masks and ventilation *Phys. Fluids* **33** 073315
[3] Dbouk T and Drikakis D 2020 On coughing and airborne droplet transmission to humans *Phys. Fluids* **32** 053310
[4] Wells W 1934 On air-borne infection: study II. Droplets and droplet nuclei. *Am. J. Epidemiol.* **20** 611–8
[5] Toossi R and Novakov T 1985 The lifetime of aerosols in ambient air: Consideration of the effects of surfactants and chemical reactions *Atmos. Environ.* **19** 127–33
[6] Qian H and Zheng X 2018 The present and future role of ultrasound targeted microbubble destruction in preclinical studies of cardiac gene therapy *J. Thoracic Dis.* **10** 1099–1111
[7] Carvalho T C, Peters J I and Williams R O 2011 Influence of particle size on regional lung deposition–what evidence is there? *Int. J. Pharm.* **406** 1–10
[8] Abuhegazy M, Talaat K, Anderoglu O and Poroseva S V 2020 Numerical investigation of aerosol transport in a classroom with relevance to COVID-19 *Phys. Fluids* **32** 103311
[9] Gu A Y, Zhu Y, Li J and Hoffmann M R 2022 Speech-generated aerosol settling times and viral viability can improve COVID-19 transmission prediction *Environ. Sci. Atmos.* **2** 34–45
[10] Kangasluoma J, Cai R, Jiang J, Deng C, Stolzenburg D, Ahonen L R, Chan T, Fu Y, Kim C, and L T M *et al* 2020 Overview of measurements and current instrumentation for 1–10 nm aerosol particle number size distributions *J. Aerosol Sci.* **148** 105584
[11] Hidy G 2019 Atmospheric Aerosols: Some Highlights and Highlighters, 1950 to 2018 *Aerosol Sci. Eng.* **3** 1–20
[12] Mainelis G 2020 Bioaerosol sampling: Classical approaches, advances, and perspectives *Aerosol Sci. Technol.* **54** 496–519
[13] Hamilton K and Haas C 2016 Critical review of mathematical approaches for quantitative microbial risk assessment (QMRA) of Legionella in engineered water systems: research gaps and a new framework *Environ. Sci.: Water Res. Technol.* **2** 599–613

[14] Guzman M I 2021 An overview of the effect of bioaerosol size in coronavirus disease 2019 transmission *The Int. J. Health Plan. Manage.* **36** 257–66
[15] Doggett N, Chow C W and Mubareka S 2020 Characterization of experimental and clinical bioaerosol generation during potential aerosol-generating procedures *Chest* **158** 2467–73
[16] Albrecht H E 2011 *Laser Doppler and Phase Doppler Measurement Techniques* (Springer)
[17] Grimm H and Eatough D J 2009 Aerosol measurement: the use of optical light scattering for the determination of particulate size distribution, and particulate mass, including the semi-volatile fraction *J. Air Waste Manage. Assoc.* **59** 101–7
[18] Whitby K T and Clark W E 1966 Electric aerosol particle counting and size distribution measuring system for the 0.015 to 1 μ size range *Tellus* **18** 573–86
[19] Garcia-Jares C, Barro R and Llompart M 2012 *Comprehensive Sampling and Sample Preparation* pp 125–61
[20] Griffiths W and DeCosemo G 1994 The assessment of bioaerosols: a critical review *J. Aerosol Sci.* **25** 1425–58
[21] Liu B Y H and Lee K W 1975 An aerosol generator of high stability *Am. Ind. Hyg. Assoc. J.* **36** 861–5
[22] von Deschwanden I, Benra F K, Dohmen H J and Brillert D 2017 PDA Measurements in Spray Generated by Twin-Jet-Nozzles *Symp.: Fluid Measurement and Instrumentation; Fluid Dynamics of Wind Energy; Renewable and Sustainable Energy Conversion; Energy and Process Engineering; Microfluidics and Nanofluidics; Development and Applications in Computational Fluid Dynamics; DNS/LES and Hybrid RANS/LES Methods) (Fluids Engineering Division Summer Meeting) (V01BT06A001)* vol 1B
[23] Ardon-Dryer K, Kelley M C, Xueting X and Dryer Y 2022 The Aerosol Research Observation Station (AEROS) *Atmos. Measurement Tech.* **15** 2345–60
[24] Horender S, Tancev G, Auderset K and Vasilatou K 2021 Traceable PM2.5 and PM10 calibration of low-cost sensors with ambient-like aerosols generated in the laboratory *Appl. Sci.* **11** 9014
[25] Rouhiainen P and Stachiewicz J 1970 On the deposition of small particles from turbulent streams *ASME Journal of Heat and Mass Transfer* **92** 169–77
[26] Haig C, Mackay W, Walker J and Williams C 2016 Bioaerosol sampling: sampling mechanisms, bioefficiency and field studies *J. Hosp. Infect.* **93** 242–55
[27] Massabò D, Danelli S G, Brotto P, Comite A, Costa C, Di Cesare A, Doussin J F, Ferraro F, Formenti P and Gatta E 2018 ChAMBRe: a new atmospheric simulation chamber for aerosol modelling and bio-aerosol research *Atmos. Measurement Tech.* **11** 5885–900
[28] Xu Z, Wei K, Wu Y, Shen F, Chen Q, Li M and Yao M 2013 Enhancing bioaerosol sampling by Andersen impactors using mineral-oil-spread agar plate *PLoS One* **8** e56896
[29] Wang S C and Flagan R C 1990 Scanning electrical mobility spectrometer *Aerosol Sci. Technol.* **13** 230–40
[30] Watson J G, Chow J C, Sodeman D A, Lowenthal D H, Chang M C O, Park K and Wang X 2011 Comparison of four scanning mobility particle sizers at the Fresno Supersite *Particuology* **9** 204–9
[31] Smolik J and Zdimal V 1993 Condensation of supersaturated vapors. Homogeneous nucleation of bis(2-ethyl-hexyl)sebacate (DEHS) *J. Aerosol Sci.* **24** 589–96
[32] Wilcox J D 1956 Isokinetic Flow and Sampling *J. Air Pollut. Control Assoc.* **5** 226–45
[33] Sousan S, Koehler K, Hallett L and Peters T M 2016 Evaluation of the Alphasense optical particle counter (OPC-N2) and the Grimm portable aerosol spectrometer (PAS-1.108) *Aerosol Sci. Technol.* **50** 1352–65
[34] Nguyen R P 2018 etudes sur les jets à contre-courant *Master in mechanical engineering* École Polytechnique de Montréal (available at: https://publications.polymtl.ca/3075/)
[35] Fuchs N A 2013 *Evaporation and Droplet Growth in Gaseous Media* (Elsevier)
[36] Froessling N 1968 On the evaporation of falling drops *Technical Report* Army Biological Labs Frederick MD
[37] Trujillo M F and Parkhill A E 2011 A local lagrangian analysis of passive particle advection in a gas flow field *Int. J. Multiph. Flow* **37** 1201–8
[38] Lewis G N and Randall M 1963 *Thermodynamics* (Krishna Prakashan Media) p 44
[39] Hamilton K A, Weir M H and Haas C N 2017 Dose response models and a quantitative microbial risk assessment framework for the Mycobacterium avium complex that account for recent developments in molecular biology, taxonomy, and epidemiology *Water Res.* **109** 310–26
[40] Biswas P, Jones C L and Flagan R C 1987 Distortion of size distributions by condensation and evaporation in aerosol instruments *Aerosol Sci. Technol.* **7** 231–46
[41] Bourouiba L 2020 Turbulent gas clouds and respiratory pathogen emissions: potential implications for reducing transmission of COVID-19 *Jama* **323** 1837–8
[42] Prussin A J, Cheng Z, Leng W, China S and Marr L C 2023 Size-resolved elemental composition of respiratory particles in three healthy subjects *Environ. Sci. Technol. Lett.* **10** 356–62